

# **In-Situ Laser Control Method for Polymer Selective Laser Sintering (SLS)**

Tim Phillips, Austin McElroy, Scott Fish, Joseph Beaman

The University of Texas at Austin  
Mechanical Engineering Department, Cockrell School of Engineering  
Austin, TX

---

## **Abstract**

Selective laser sintering (SLS) of Nylon is a significant portion of the Additive Manufacturing (AM) market for structurally sensitive applications. To achieve high performance in these laser melted parts, one would like to see consistent melting of the powder over the part region in each layer of the build. Current research methods into improving this consistency focus on the use of IR sensing to adjust heating elements in attempt to gain even temperature distributions over the pre-laser melted powder layer with the expectation that the laser at constant power, speed, spot size, and spacing will deliver constant melting properties. In this paper we examine a complimentary method of gaining even melted properties by sensing the pre-lased powder along the laser track, and adjusting the laser power to achieve a common post melted temperature everywhere on the part. We describe the feedback based laser control method that varies the laser power in to account for the pre-sintering temperature profile across the part bed. Various tests have been performed, and a method for employing this strategy throughout a build is presented.

---

## **Introduction**

Selective Laser Sintering (SLS) is an additive manufacturing process that creates 3D parts by sintering powdered material, in this case nylon, together with a laser. To create a 3D SLS part, the computer aided design (CAD) model is sliced into a stack of 2D cross-sections, typically 0.004 inches thick each. To begin building a part, the SLS machine uses radiative and conductive heaters to heat the surface of the nylon powder to just below the melting temperature. Once the powder's temperature has stabilized, the laser will scan the powder in a pattern defined by the first 2D cross-section. Following this, a new layer of powder is spread, heated, and fused in the pattern of the next 2D cross-section. This process is repeated until all cross-sections have been sintered and the final 3D part is formed.

This process is heavily dependent on the thermal profile of the nylon powder and excess temperature gradients both laterally and in depth can induce curling of the part during the build or inadequate mechanical and dimensional properties [1]. A typical process control objective is to bring the powder to a consistent temperature of around 182°C for Nylon 12, just a few degrees below the melting point of the powder [2]. Once this temperature has stabilized, the laser scans, using just enough laser power to fully sinter the layer. This ensures that temperature gradients are kept to a minimum. Previous research has examined the design and control of heater systems attempting to maintain small temperature gradients across the powder surface [3] [4]. These

systems have reduced, but not eliminated thermal gradients in the pre-scanned powder and further improvement is needed to provide consistent/predictable part properties.

Other factors that affect the thermal profile of the powder are part geometry and laser scan pattern. While nylon powder is a good thermal insulator, heat still dissipates between layers. This means that in instances where the current layer being sintered has regions beneath it that vary in amount of sintering, such as when creating an unsupported overhang, thermal gradients can arise.

The most basic laser scan pattern consists of straight lines that overlap slightly along their axis, meaning that the first few lines have less overlap with previously sintered lines when compared to lines in the center of the part. This can be seen in Figure 1, where three rectangular part sections are being scanned with a fill pattern, and the first 3 vector scans are cooler than the later 8 scan lines. This figure also shows hot spots at the beginning and end of the scan lines due to inadequate galvanometer tuning.

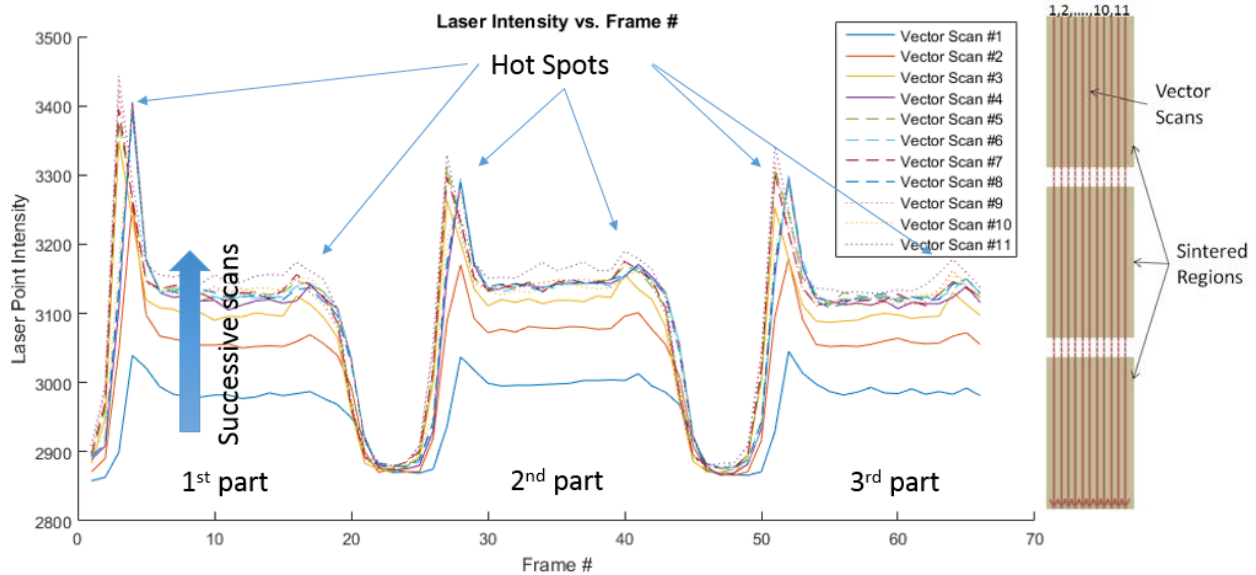


Figure 1: Laser Scan Line Temperature

In an open loop system, these influences on powder temperature are unaccounted for and can decrease the quality of the final part. When a constant laser power is used along a scan line, the sintered powder will largely all experience the same temperature increase (disregarding end of vector over-sintering caused by inadequate galvanometer tuning). This means that any temperature gradient that exists in the powder initially will be preserved after sintering. The resulting part also contains this temperature gradient which can cause the part to curl or can cause unpredicted geometrical and structural characteristics. By controlling the post-sintering temperature of a part and decreasing the variation among post-sintering temperatures, part quality and predictability can be increased [5]. Post-sintering temperature monitoring [6] and control [7] has been explored previously for metal additive manufacturing processes, but little has been done to control post-sintering temperatures in polymer SLS.

## Experimental Setup

### Testbed

In-situ laser power compensation using closed-loop feedback was accomplished on the Laser Additive Manufacturing Pilot System (LAMPS), seen in Figure 2. LAMPS is an open hardware SLS platform that was designed and built at the University of Texas at Austin as an experimental testbed for SLS process control. LAMPS uses a 60 watt CO<sub>2</sub> laser with a Cambridge Technologies EC1000 laser and galvanometer controller. The build surface is 220 mm x 220 mm and sintering takes place in a heated nitrogen atmosphere. The machine utilizes independently controlled strip heaters to heat the walls of the build chamber which, in turn, control the atmosphere temperature. The strip heaters do the majority of the work heating the powder and additional quartz lamps are used to fine tune the temperature as well as to do the fast heating required after new powder is spread. All measurement and control is handled through National Instruments Labview software and cRIO hardware.

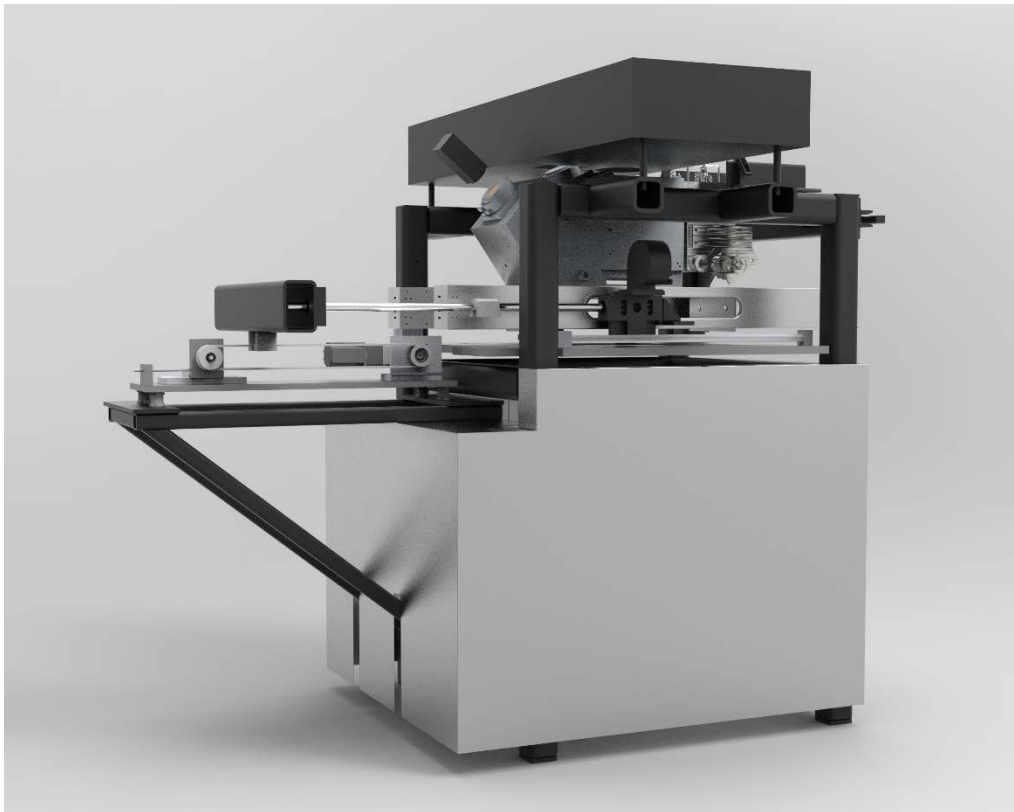


Figure 2: LAMPS rendering

### Infrared Camera Capability

In addition to atmosphere feedback via thermocouples, LAMPS uses two infrared (IR) cameras to monitor and control the building process. A FLIR A325 Long Wave Infrared (LWIR) camera is held in a stationary position and directed at the build surface. This camera provides feedback to control the duty cycle of the quartz lamps. This allows for control of the powder surface temperature as each layer is spread in preparation for laser melting. The second IR camera is a FLIR SC8240 Mid Wave Infrared (MWIR) camera. This is a high-speed IR camera capable of recording 2,243 frames per second at 64x64 pixels per frame. This camera is boresighted with the CO<sub>2</sub> laser, providing a constant view of the build surface in the immediate

vicinity of the scanning laser contact point. This is accomplished by placing a dichroic mirror in the laser path before the galvanometer system, as seen in Figure 3. Since this is done prior to the optical path entering the galvanometer system, the field of view (FOV) of the MWIR camera will not be stationary and will follow the laser as the galvanometer scans across the powder surface. The result is a close up view of the powder surface with the laser spot centered in the image, regardless of position on the build surface.

An image taken with the MWIR camera is presented in Figure 4. The color bar shown in the image is in units of “count”, which is a measure of the amount of photons reaching the camera’s sensor during the integration period. It is possible to convert this unit to temperature, but it is highly dependent on parameters such as transmittance of the optics, emissivity of the powder, reflected radiation, and other parameters that are not known precisely. Since counts can be related to temperature however, and our interest is in creating consistency and temperature, the counts can be used directly in the feedback control. To give the reader a sense of scale, 7900 counts is roughly equal to 177°C and a 400 count change is equal to a change of roughly 3.8°C.

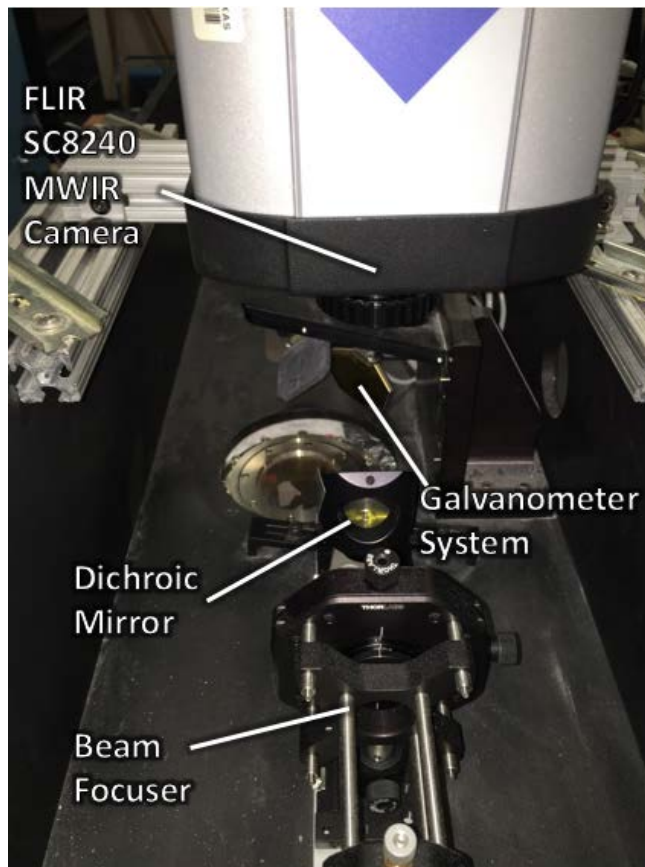


Figure 3: Boresight IR Camera Setup

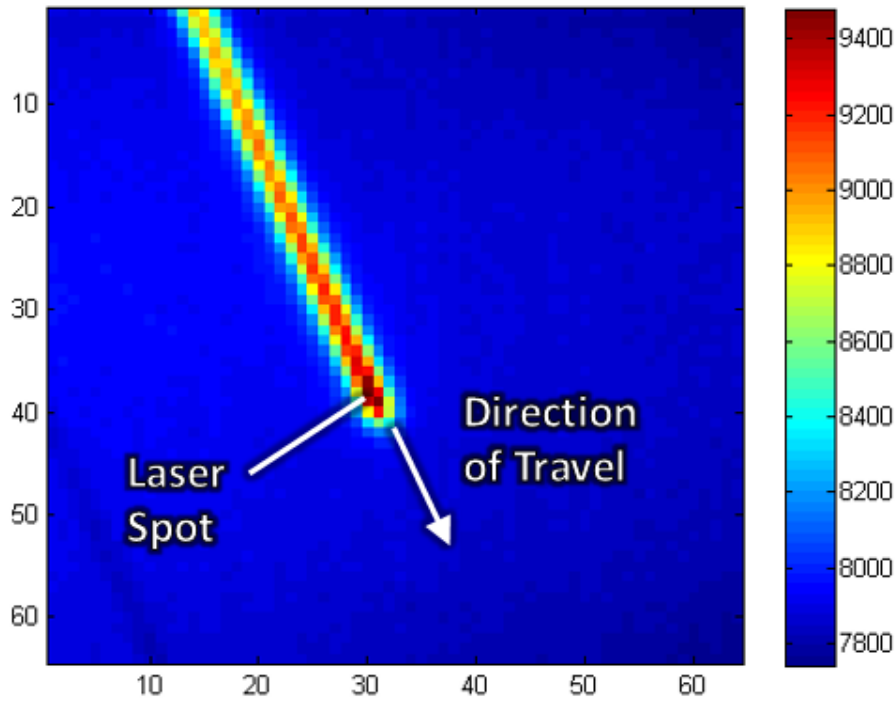


Figure 4: MWIR Camera View

### Control Strategy

The results presented in this paper employ the strategy described here to create individual laser scan lines. By repeating this process, multiple scan lines can be positioned and overlapped, creating an entire 3D part with excellent control of the post-sintering temperature of the part. This in-situ laser compensation strategy employs a multiple scan approach that is separated into two phases. In the first phase, the galvanometers scan the MWIR camera and laser across the build surface in the same fashion as if it were sintering a layer, except with the laser turned off. During this phase, the MWIR camera is used to record powder temperature where the laser will sinter, giving the initial temperature gradient of the powder. This temperature gradient is analyzed and used to develop a laser power profile for sintering that will produce a scan line with a consistent post-sintering temperature, regardless of the temperature gradient present initially.

The second phase is to employ the scan strategy developed in the first phase to sinter the scan line with variable power. The MWIR camera continues to record data in this phase and is used to verify the post-sintering temperatures.

### Hardware Limitations

The ultimate goal of this technology is to implement a real-time control method, where the system can acquire feedback and vary the laser power in real time during a laser scan. Current hardware compatibility limitations, described below, prohibit real-time control for this experiment so results presented in this paper focus on in-situ control. The compatibility issues will be addressed in future effort and publications.

One current limitation to using a variable laser power is with the laser controller. LAMPS uses a Cambridge Technologies EC1000 controller for the laser and galvanometer system. The EC1000 only allows a fixed power to be used for each laser scan line, meaning a line must be broken into subsections and each fed separately to the EC1000 in order to use different amounts of laser power in different areas of the original scan line. Another limitation is the framerate of the MWIR camera. While it records at a high framerate of 2,243 frames per second, a framerate greater than 4,000 frames per second would be needed to sample each voxel of powder [8].

As mentioned previously, the machine control is implemented using LabVIEW and incorporating the MWIR camera into the LAMPS control program was not completed for this experiment. The host computer is not fast enough to handle the control program simultaneously with the high data rate MWIR data acquisition. The interim solution was to use a separate computer for recording and analyzing the MWIR data and manually transferring the scan strategy to the LAMPS control computer to actuate the laser. This resulted in a delay of approximately two minutes between acquiring the initial temperature gradient and actuating the laser, hence the inability to do real-time control. This is also the reason the results here are limited to individual scan lines, as doing multiple lines would change the temperature gradient and phase one of the control strategy would have to be repeated before every scan line. By incorporating the MWIR camera and LAMPS control software on the same computer, though, it would be possible to use this control strategy to build an entire 3D part. The objective here is to show feasibility and benefits of the general approach, even with these current limitations.

## Results

### Baseline Fixed-Power Results

One assumption made was that using a fixed laser power would preserve the initial temperature gradient. To verify this assumption, the MWIR camera was scanned across a laser scan line before and during sintering to record temperatures of where the laser sintered. Figure 5 shows these results for scanning a line with 10% laser power. The green line is the temperature before sintering and the blue line is the temperature after. To better visualize how the post-sintering temperature is affected by a constant laser power, the second subplot shifts the pre-sintering temperature upwards by a constant values so that the beginning of the scan lines coincide. This clearly shows that the temperature profile is the same for both lines, meaning it was unaffected by the constant laser power sintering. Figure 6 shows the results of a similar test, this time with a scan line split into two subsections with each subsection receiving a different laser power. Again, this shows that the pre-sintering temperature profile has been preserved and the assumption is valid.

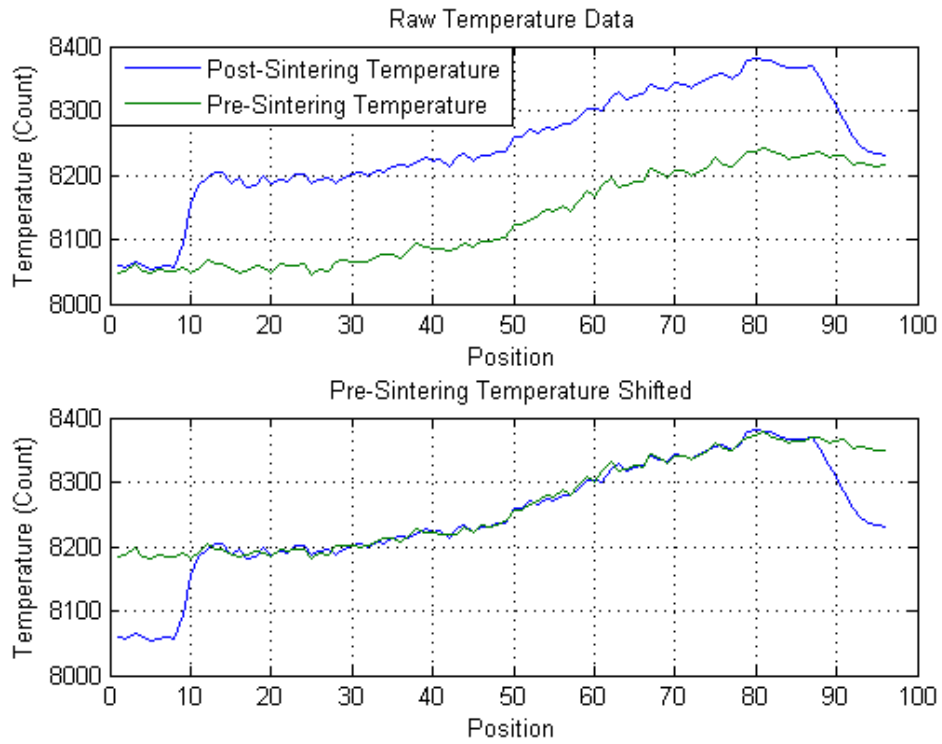


Figure 5: Temperature Comparison at 10% Laser Power

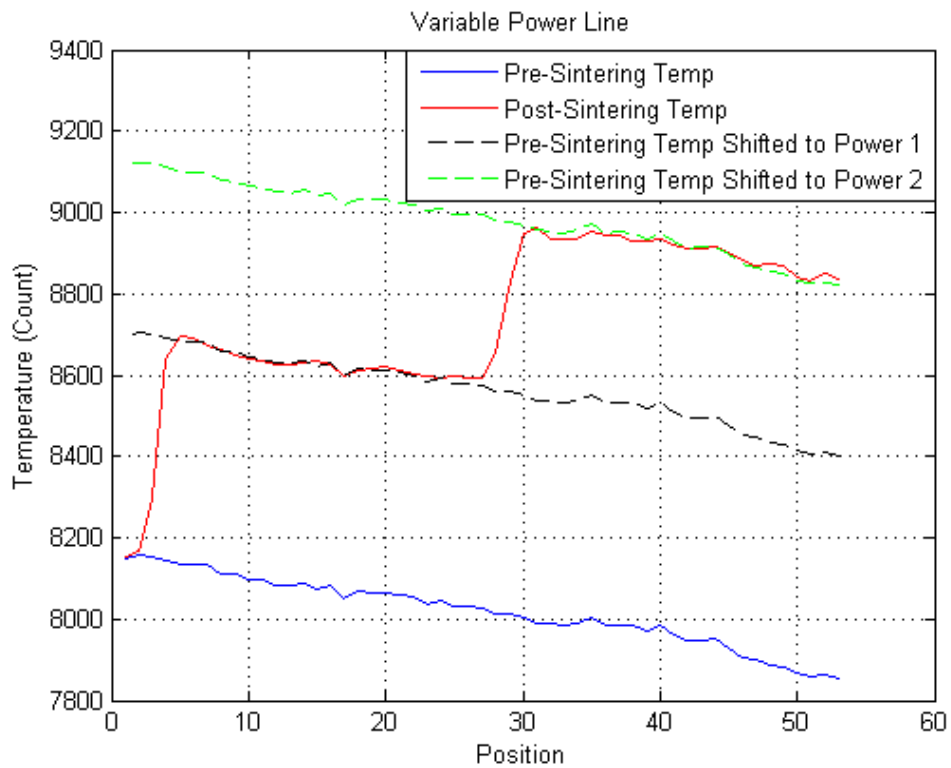


Figure 6: Temperature Comparison with Variable Laser Power

To accurately control the post-sintering temperature, a transfer function between applied laser power and post-sintering temperature increase must be created. To do this, multiple lines were sintered using different laser powers and their pre- and post-sintering temperatures were compared. The result of one of these tests is seen in Figure 7. Once these tests were performed, the results were compiled and a best-fit line was found that would provide the equation for desired temperature increase and delivered laser power. This can be seen in Figure 8, where some outliers in the data were removed and the resulting 4<sup>th</sup> order polynomial fit line has an R<sup>2</sup> value of 0.9988. Note that this figure shows 5% laser power results in no temperature increase. This is because that is near the threshold value for laser power, below which the laser does not fire.

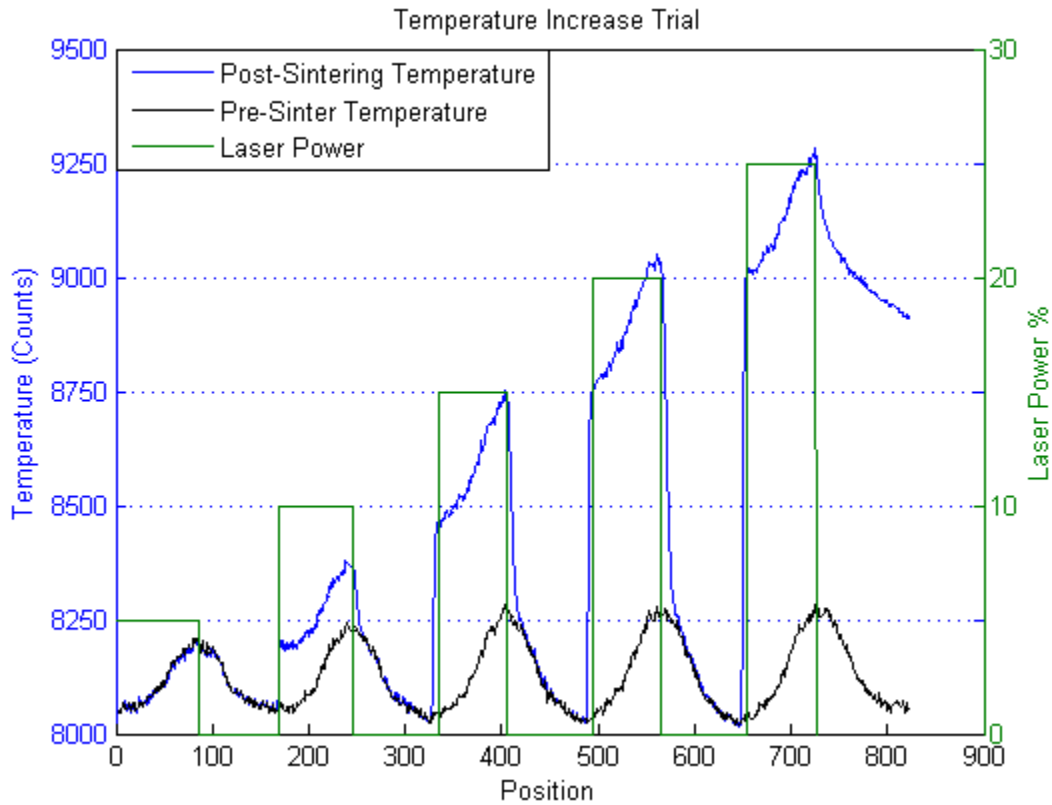
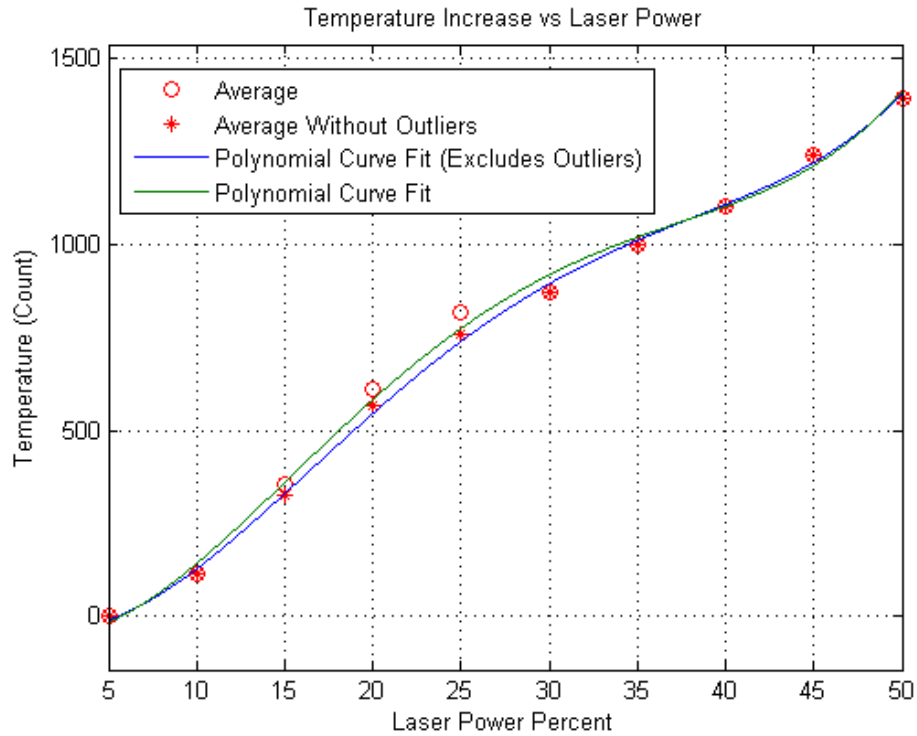


Figure 7: Laser Power and Temperature Increase Trial





**Figure 8: Temperature Increase vs. Laser Power**

Some baseline testing was conducted using a fixed laser power, the results of which will be compared with the results of the in-situ control method presented. The raw data is shown in Figure 9 which shows a dwell time at the beginning of the test before the galvanometers begin moving, a temperature rise as the galvanometers move to the start of the scan line immediately followed by a temperature decrease as the galvanometers scan across the line with the laser off. This is immediately followed by a temperature decrease as the galvanometer moves back to the start of the scan line then a large jump in temperature as the laser is turned on and the line is scanned. This is followed by another dwell time as the galvanometer rests at the end of the scan line with the laser turned off and the powder can be seen cooling. Trimming this data to just show the two sections where the galvanometers are scanning forwards across the scan line (once with the laser off, once with it on) is seen in Figure 10 where the data is shifted in the x-direction such that the pre- and post-sintering temperatures are lined up with their position in the build chamber. The results of the three baseline tests are quantified in Table 1.

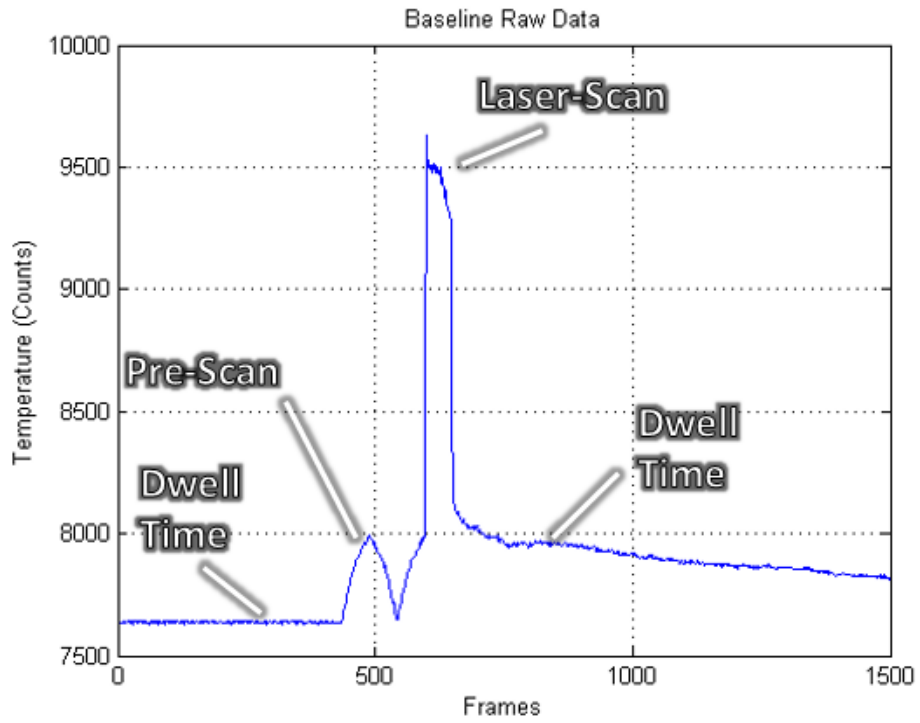


Figure 9: Raw Baseline Temperature Data

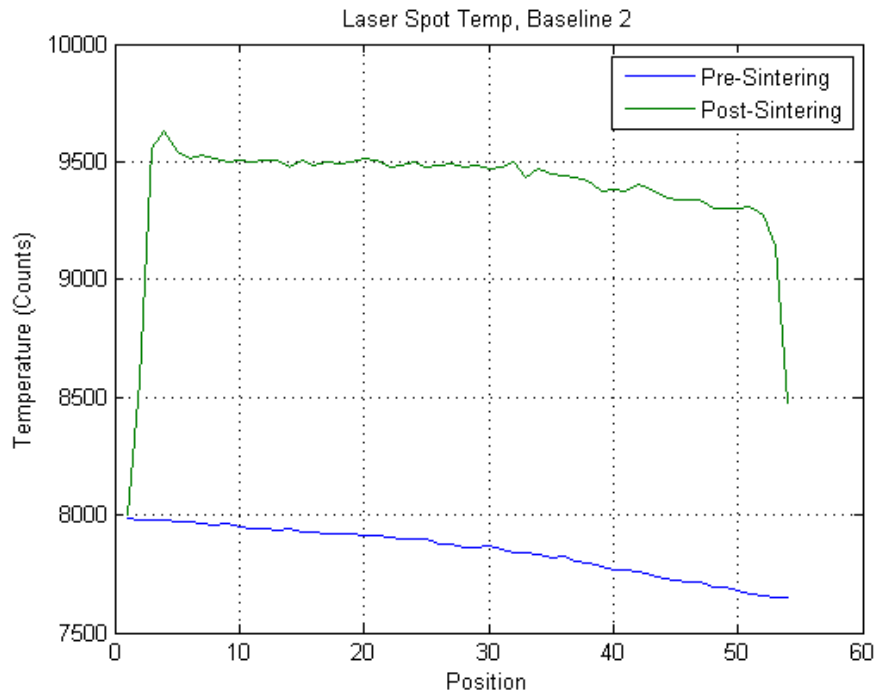


Figure 10: Baseline Temperature Data

Table 1: Baseline Temperature Measurements, Measured in Photon Count

Trial	Avg. Pre-Sintering Temp.	Max Pre-Sintering Temp Difference	Pre-Sintering Temp STD	Avg. Post-Sintering Temp	Max Post-Sintering Temp Difference	Post-Sintering Temp STD	Temp Diff Change	Temp STD Change
1	8022.6	291	88.6	9584.1	522	89.5	-79.38%	-1.02%
2	7843.7	314	93.2	9442.4	256	73.2	18.47%	21.46%
3	7751.7	316	97.8	9292.1	414	75.8	-31.01%	22.49%

### In-Situ Laser Power Compensation

In-situ control of laser power was performed as described in the control strategy section. The result of phase one of the control strategy, where the pre-sintering temperature profile is acquired, for one of the in-situ control trials can be seen in Figure 11. With a goal of a post-sintering temperature of 9,000 counts, this temperature profile was fed through the laser power to temperature increase transfer function. The result of the transfer function is seen in Figure 12. Each time the laser power is changed a new line subsection must be created. To keep the number of line subsections manageable, the laser power percentage was limited to integer values. If the laser controller was capable of modifying laser power mid-scan line, this would look like a smooth function rather than a step-wise function.

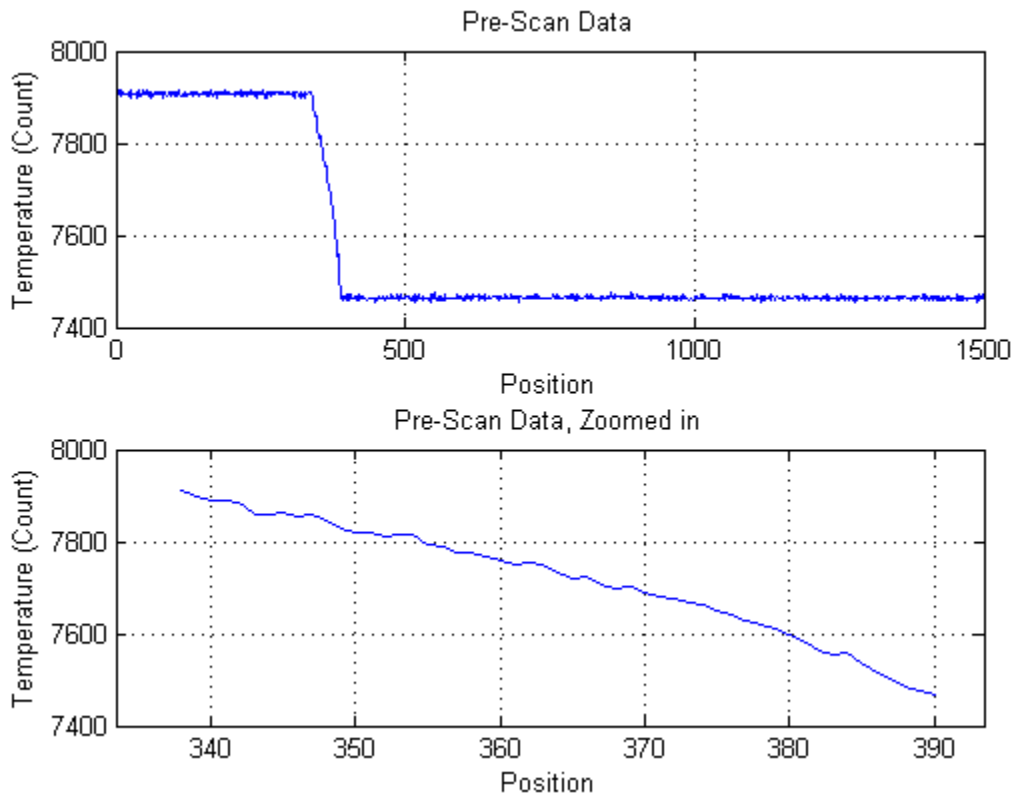


Figure 11: Pre-Sintering Temperature Profile

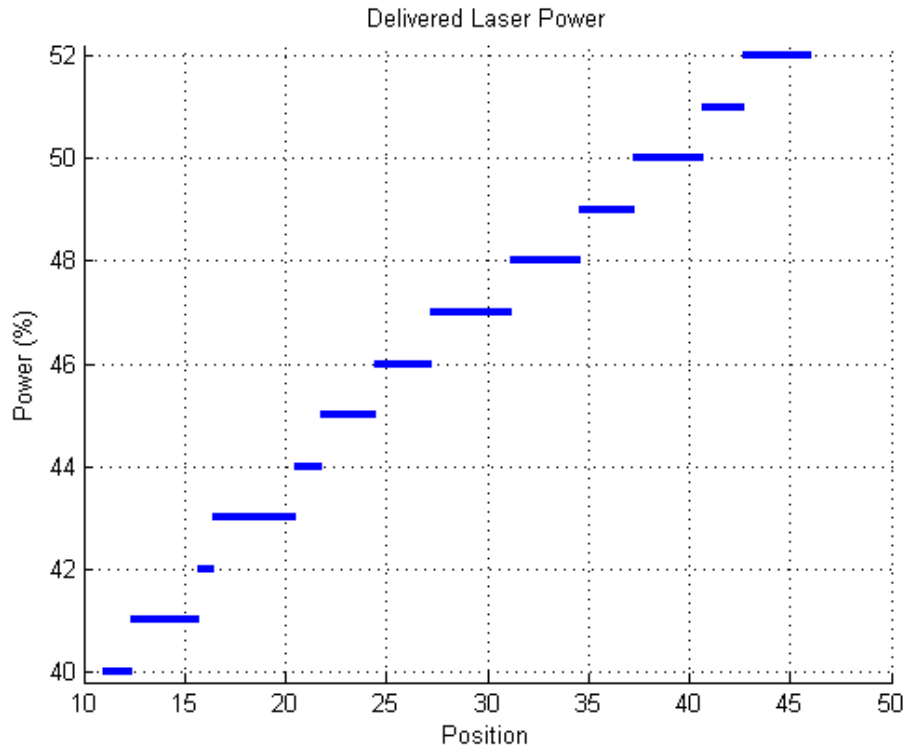


Figure 12: Delivered Laser Power

The scan strategy detailed in Figure 12 was implemented and the results can be seen in Figure 13. In this image, the red line represents the same data seen in Figure 11 and is the temperature profile that is used to compute the laser power profile. Once the laser power profile is developed, it is fed back through the laser-power-to-temperature-increase transfer function to get a projected temperature increase. This temperature increase is added to the initial temperature profile to get a projected post-sintering temperature profile, which is shown in black. Note that this is not a straight line at 9,000 counts because only integer laser power settings were used as discussed above.

The process of analyzing the initial temperature profile, developing a laser power profile, and preparing the laser to implement said power profile takes approximately two minutes due to the restrictions detailed in the hardware limitations section. Immediately prior to the variable laser power scan line, the galvanometers scan the line again with no laser power. The result of this is shown in blue. The purpose of this step is to ensure that the initial temperature of the scan line has not changed in the two minutes it took since the initial data was taken. If the red and blue lines are significantly different, the system has changed and it is expected that the laser power profile developed would not produce the desired results. In this case, the red and blue lines are in close agreement, so the actual post-sintering temperature, shown in green, is expected to match closely with the projected post-sintering temperature shown in black. This figure shows a successful trial as the post-sintering temperature was well controlled and is not influenced by the initial temperature profile of the powder.

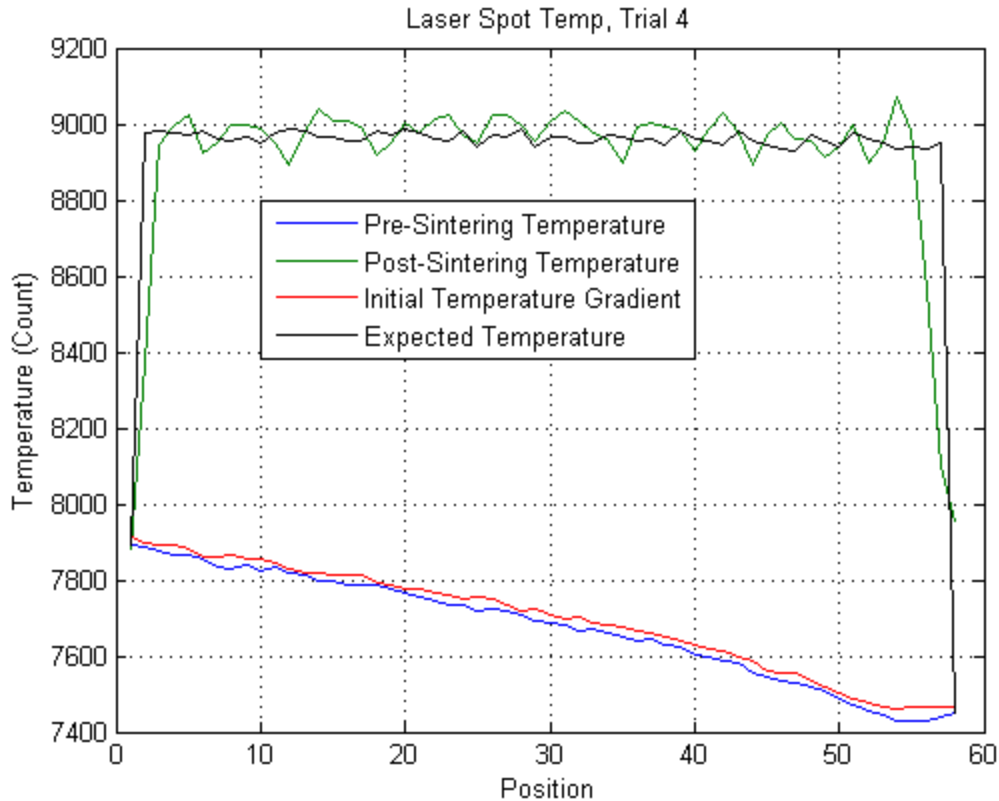


Figure 13: In-Situ Laser Control Results for Trial 4

Not all trials were as successful, as can be seen in Figure 14. This trial shows overcompensation by the laser as the post-sintering temperature increases over the length of the scan line. One explanation for this result is that this trial was performed at the lowest power level and it is possible that the laser power to temperature increase transfer function was not as accurate in this region. The results of all closed-loop trials are quantified in Table 2. Note that this table is missing data for trials 3, 8, and 13, which contained MWIR camera recording errors or errors found after the test in one of the MATLAB scripts used to create the variable laser power scan files. These are all errors in the implementation of control, not flaws in the control method and do not detract from the validity of the in-situ laser compensation strategy presented. While a few of the trials produced less-than-optimal results, all trials outperformed the baseline trials and were successful in decreasing the variation in the post-sintering temperature when compared to an open-loop, fixed laser power system.

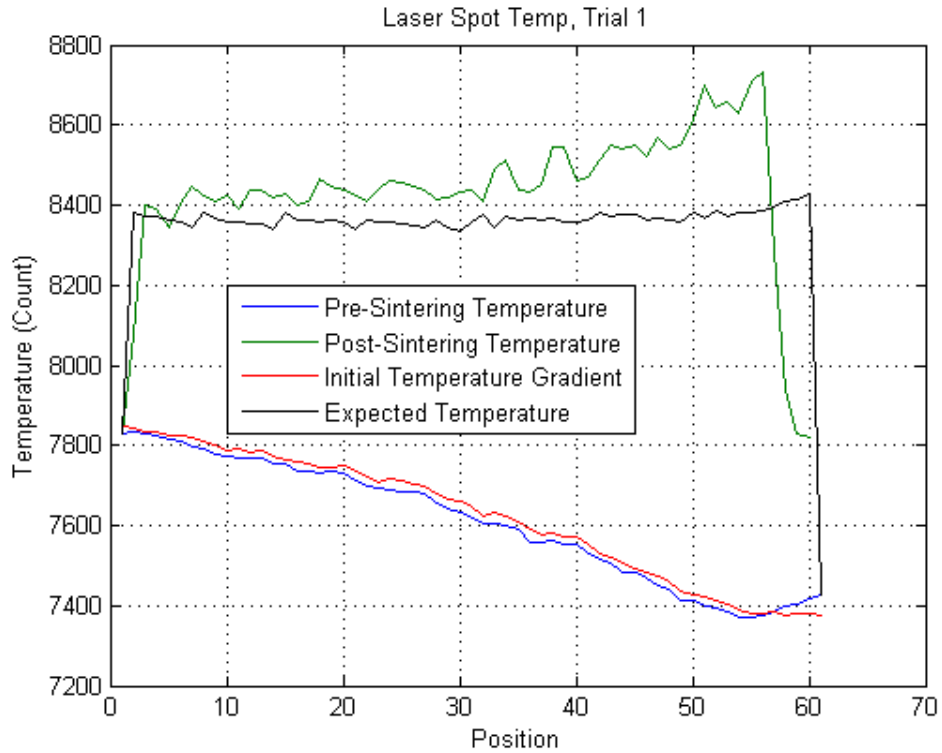


Figure 14: Laser Power Overcompensation

Table 2: In-Situ Control Temperature Measurements

Trial	Avg. Pre-Sintering Temp.	Max Pre-Sintering Temp Difference	Pre-Sintering Temp STD	Avg. Post-Sintering Temp	Max Post-Sintering Temp Difference	Post-Sintering Temp STD	Temp Diff Change	Temp STD Change
1	7612.3	457	142.2	8482.8	389	89.3	14.9%	37.2%
2	7629.2	402	126.0	9083.6	210	42.0	47.8%	66.7%
3	--	--	--	--	--	--	--	--
4	7682.4	439	124.5	8978.1	183	40.8	58.3%	67.2%
5	8018.4	326	96.6	8901.6	149	31.6	54.3%	67.3%
6	7768.9	377	114.6	9042.1	245	68.4	35.0%	40.3%
7	7677.3	374	110.2	9292.4	250	52.9	33.2%	52.0%
8	--	--	--	--	--	--	--	--
9	7663.7	396	112.2	8953.3	191	45.3	51.8%	59.6%
10	7610.4	385	114.8	8988.2	258	60.9	33.0%	47.0%
11	7575.1	391	116.4	8931.2	303	79.8	22.5%	31.4%
12	7745.0	355	103.0	8761.0	124	24.2	65.1%	76.5%
13	--	--	--	--	--	--	--	--

## Conclusion

The hypothesis that a traditional, fixed laser power sintering method would uniformly increase the temperature of powder and preserve pre-sintering temperature gradients was confirmed. This revealed the need for an improved laser control method that could compensate for initial temperature gradients and produce sintered regions with little temperature variation. The method proposed used an infrared camera to measure the pre-sintering powder temperature and compute an appropriate laser power needed to produce the desired post-sintering temperature. This regulated the laser power delivered in order to counteract the initial thermal profile of the powder to produce a uniform post-sintering temperature.

The results are overwhelmingly positive, with each trial outperforming the baseline open loop system. The control strategy presented in this paper saw reductions in the influence of the pre-sintering temperature profile of up to 65%. This increased control over post-sintering temperatures has the capability of improving the mechanical and dimensional properties of SLS parts [5], as well as increasing the repeatability of the sintering process.

Future work involves applying the control strategy presented to an entire 3D part using real-time control. This will involve further automation in developing the laser power profile for each scan line. It would also be beneficial to have an automated process for developing the laser power to temperature increase transfer function. This process could be performed periodically to ensure the delivered laser power is still expected to produce the same temperature increase. Periodically updating the transfer function is likely to increase the amount of control over the post-sintering temperature. Another avenue for further exploration is to adapt this in-situ control strategy into a real-time control strategy. This will likely involve additional hardware and software that operates quickly and is capable of varying the laser power in real-time without the need to split the scan line into subsections.

## Bibliography

- [1] J. A. Benda, "Temperature-Controlled Selective Laser Sintering," in *Solid Freeform Fabrication Symposium*, Austin, 1994.
- [2] P. Hall, Interviewee, *SLS Process Overview*. [Interview]. 2015.
- [3] D. L. Bourell, T. J. Watt, D. K. Leigh and B. Fulcher, "Performance Limitations in Polymer Laser Sintering," *Physics Procedia*, pp. 147-156, 2014.
- [4] W. W. Wroe, "Improvements and Effects of Thermal History on Mechanical Properties for Polymer Selective Laser Sintering (SLS)," University of Texas, Austin, Austin, 2015.
- [5] J. R. Rajan and K. L. Wood, "Experimental Study of Selective Laser Sintering of Parmax," The University of Texas at Austin, 2001.
- [6] Y. Chivel and I. Smurov, "On-line temperature monitoring in selective laser sintering/melting," *Physics Procedia* 5, pp. 515-521, 2010.
- [7] S. Clijsters, T. Craeghs, S. Buls and K. Kempen, "In situ quality control of the selective laser melting process using a high-speed, real-time melt pool monitoring system," *Int J Adv Manuf Technol*, vol. 75, pp. 1089-1101, 2014.
- [8] G. M. Koretsky, J. F. Nicoll and M. S. Taylor, "A Tutorial on Electro-Optical/Infrared (EO/IR) Theory and Systems," Institute for Defense Analyses, 2013.